Int. Journ. of Unconventional Computing, Vol. 19, pp. 1–15
Reprints available directly from the publisher
Photocopying permitted by license only
DOI: 10.32908/ijuc.v19.200823

Light-Sensitive Diffusion Diodes for Reaction-Diffusion Waves

CHASE A. FULLER[1,2], DANIEL COHEN-COBOS[1], JOHN F. LINDNER[1,3] AND NIKLAS MANZ[1,*]

[1]*Department of Physics, The College of Wooster, Wooster, OH 44691, USA*
[2]*Department of Physics and Astronomy, University of Iowa, Iowa City, IA 52242-1479, USA*
[3]*Department of Physics, North Carolina State University, Raleigh, NC 27695-8202, USA*

Received: August 19, 2023. Accepted: August 24, 2023.

We use the Tyson-Fife model of the Belousov-Zhabotinsky reaction to numerically investigate the propagation of chemical reaction-diffusion waves through narrow, quasi-one-dimensional channels. We create soft obstacles in the form of activator and inhibitor diffusion coefficient inhomogeneities. Using a Fast Inhibitor Diffusion Region, in which the inhibitor's diffusion is larger than the activator's diffusion, the system can exhibit unidirectional propagation behavior – the diffusion diode. In a light-sensitive BZ-system, we discover a nonlinear compensation relationship between a higher activator diffusion (causing increased wave speed) and illumination (causing decreased wave speed) to achieve normal wave behavior. This enables the creation of a very energy efficient on/off-switch for chemical computation circuits in which a low intensity light pulse can be applied to a diffusion diode to disable wave propagation.

Keywords: Barkley model, Belousov-Zhabotinsky reaction, diffusion coefficient, Diode effect, fast inhibitor diffusion region, fast propagation region, light-sensitivity, nonlinear wave, numerical simulation, reaction-diffusion wave, Tyson-Fife model

1 INTRODUCTION

Nonlinear dynamical systems outside of thermodynamic equilibrium reveal a fascinating wealth of spatial, temporal, and spatio-temporal structures on a macroscopic scale in various physical, chemical, and biological

* Contact author: E-mail: nmanz@wooster.edu

pattern-forming systems. In excitable reaction-diffusion (RD) media [19], propagating fronts are also the building blocks of more complex spatio-temporal patterns. The Belousov-Zhabotinsky (BZ) reaction has become a model system to investigate excitable media because of the wide variety of options to interfere with its wave behavior by manipulating the reaction and/or the diffusion component, creating inhomogeneous conditions.

These options include, for example, light-sensitivity [12, 23], geometrical constrains [37], temperature [24], electric fields [35], kinetic modulations [21], non-penetrable no-flux boundary (hard) obstacles [6], or soft obstacles [51]. It is also possible to create diffusion inhomogeneity, allowing the excitation front to enter and propagate under different conditions than on the outside [52]. A comparison of the effect between similar soft and hard obstacles has been investigated by Tanaka *et al.* [39]. Soft obstacles can effect the reaction and/or the diffusion of a propagating wave. The photosensitive RD system is mostly used to manipulate the reaction aspect, whereas liquid media with gel-like obstacles can be used for manipulating the diffusion aspect without interfering with the reaction term. The interface between a liquid solution and a gel creates a diffusion step similar to a fast propagation region [31]. It has also been shown that waves passing through two unequal holes [30] or interactions with obstacles [32, 50] can initiate spiral waves which are of interest in chemical computing (pulse generator) and cardiac research (fibrillation of the heart).

The spatial geometry and homogeneity within the soft obstacle areas has a significant effect on the overall wave behavior. For example, if the obstacle is a homogeneous, non-excitable area, excitation waves can tunnel through those obstacles [31]. In particular, Gao *et al.* examined the effect of Fast Propagation Regions (see, for example [52]) with a modified Barkley model [7] which can, in particular configurations, initiate an unidirectional block of the wave propagation or create rotating spirals [11]. A review about wave propagation in inhomogeneous excitable media can be found in [51]. Ermentrout and Rinzel used a structural inhomogeneity (change in wire diameter) to create a system in which a signal can be blocked, passed, or reflected [9].

The large variety of geometrical and RD-specific manipulations in one- and two-dimensional geometries are the basis for the idea that excitable systems can be used for information processing which is also called ‘chemical computing’ [3, 14–16]. Besides general mathematical procedures as they appear in classical computers or signal manipulations in nerves, language recognition systems have also been created [8]. Examples of classical computing using BZ systems are logic gates [44], multi-bit binary adder [49], or multi-bit binary decoder [38].

Initially, unidirectional behavior in wave propagation was the result of a non-parallel gap between two excitable area (e.g., corner of one square

touching the side of another) [4], perpendicular channels touching each other [33], or asymmetric connections [18, 34]. Another option is the connection of a narrow channel to a wide 2D area [42]. In branching systems, the angle between the channels plays a role as well [2], as does a set of gaps [5]. Using an illumination gradient, it was computationally shown [43] and later experimentally verified [17] that unidirectional propagation is possible. An excitation wave could travel in one direction across an illumination gradient, but not the other. Similar results were found with a step-barrier composed of two areas with different but homogeneous excitabilities [13].

Experimentally, the diffusion properties of RD waves can be manipulated in many ways. The first developed method were catalyst-loaded beads which are immersed in a catalyst-free aqueous BZ solution [27, 28]. Those beads are coupled mostly via diffusion of the activator molecule $HBrO_2$. Another option are BZ-vesicles in water-in-oil microemulsions, coupled by diffusion of the inhibitor molecule Br_2 through the oil phase [41, 48]. Very recently, spherical silica gel BZ microparticles have been used in which the BZ reactants are confined inside these beads [25, 26].

Computational studies of reaction-diffusion systems afford control over parameters and conditions that are difficult to control in the lab. With the already healthy agreement between mathematical models and observed dynamics [51], we can comfortably interrogate the effects of precisely varying such parameters. Of late, inhomogeneous variations have been of interest, see for example Kozak *et al.* [21].

In this study, we focus on inhomogeneous diffusion in the Tyson-Fife model of the Belousov-Zhabotinsky (BZ) reaction. We investigate the effect of the channel's diffusion condition on wave propagation. But instead of implementing Fast Propagation Regions (FPR), with an increased activator diffusion coefficient D_u and, most of the time, immobilized inhibitor diffusion coefficient D_v, we implement a Fast Inhibitor Diffusion Region (FIDR), increasing the inhibitor diffusion coefficient to obtain a diffusion ratio of $D_v/D_u > 1.0$. Totz *et al.* used FIDR to observe transversal wave front instabilities instead of the usual damping of curvature perturbations [45]. Section 2 describes our mathematical model, Section 3 describes our numerical methods, Section 4 details our diffusion diodes and light-sensitive switches, and Section 5 offers our conclusions.

2 MODEL

Excitable reaction-diffusion systems, in general, share some kind of activator species u and inhibitor species v whose interplay produces the rich dynamics these systems are known for. The reaction part of our reaction-diffusion

system is the Tyson-Fife [47] reduction of the three-variable Oregonator model [10]

$$R_u[u, v] = \frac{1}{\epsilon}\left(u - u^2 - f v \frac{u - q}{u + q}\right) \tag{1a}$$

$$R_v[u, v] = u - v \ , \tag{1b}$$

where $\epsilon \ll 1$ is a scaling parameter, and f and q are chemical parameters. These two equations represent the coupled change in the two dimensional concentration of the activator $u[x, t]$ and inhibitor $v[x, t]$ over space x and time t due to the chemistry of the BZ reaction.

For the parts of our investigation in which we applied illumination as another modulating parameter on the wave propagation, we followed Krug *et al.* [22] and included the photoinhibitory term ϕ into Eq. (1a) to obtain

$$R_u[u, v] = \frac{1}{\epsilon}\left(u - u^2 + (f v + \phi)\frac{q - u}{q + u}\right) \tag{2a}$$

$$R_v[u, v] = u - v \ . \tag{2b}$$

For spatially varying diffusion coefficients we need to use Fick's Second Law for variable diffusion of a species w, which implies the generalized diffusion equation

$$\begin{aligned} \partial_t w &= \vec{\nabla} \cdot \vec{J_w} = \vec{\nabla} \cdot \left(D_w \vec{\nabla} w\right) = \vec{\nabla} D_w \cdot \vec{\nabla} w + D_w \nabla^2 w \\ &= \partial_x D_w \, \partial_x w + D_w \partial_x^2 w \end{aligned} \tag{3}$$

in $1 + 1$ dimensions. The above formulation is general: we recover homogeneous diffusion when the diffusion coefficients are constants, as the gradient of a constant is zero and so the gradient-product term collapses.

Once assembled, the Tyson-Fife reaction-diffusion system with spatially dependent diffusion coefficients reads

$$\partial_t u = R_u + \partial_x D_u \, \partial_x u + D_u \partial_x^2 u, \tag{4a}$$

$$\partial_t v = R_v + \partial_x D_v \, \partial_x v + D_v \partial_x^2 v. \tag{4b}$$

The system is ready for the application of numerical techniques.

3 NUMERICAL METHODS

To guard against error, we implement two independent numerical pipelines: the Finite Difference Method (FDM) in Obj-C and the Finite Element Method (FEM) in Mathematica [1].

For FDM, we apply a Forward-Time-Central-Space finite differencing method to our system of equations with no-flux, Carl Neumann boundary conditions [29] to contain the simulation. Continuous time and space are discretized to have small but finite space Δx and time Δt steps. We evolve forward in time by substituting finite approximations for the derivative operators. Numerical error are bounded for $\Delta t \ll \Delta x^2$. FDM integration steps are typically $\Delta t = 0.001$ and $\Delta x = 0.15$. A more detailed description can be found in Smith *et al.* [36].

As an FEM check, we also use Mathematica's `NDSolve[]` function to implement the method of lines. Spatial discretization is via finite elements with a maximum mesh cell size of 0.2.

For all our simulations, we use the parameters $\epsilon = 0.03$, $f = 3.0$, and $q = 0.001$ in Eq. (1a) if not otherwise stated. Under normal channel conditions, without any diffusion diode, we use $D_v = D_u = 0.5$.

4 RESULTS

4.1 Diffusion Diode Behavior

Zykov *et al.* reported unidirectional propagation or diode behavior in a two-step fast propagation region with no inhibitor diffusion [52]. Under these conditions, a wave is blocked by a very sharp increase in the activator's diffusion rate whereas the wave propagates though this region if the step height is divided into two steps of half-height (see Figure 1 of [52]).

In contrast, Eqs. (4) consider activator *and* inhibitor diffusion and we use the ratio of the inhibitor diffusion coefficient to the activator diffusion coefficient D_v/D_u to define the region. In a Fast Inhibitor Diffusion Region (FIDR), with diffusion ratio $D_v/D_u > 1$, wave death is possible, and we observe unidirectional propagation caused by sufficiently large inhibitor diffusion D_v.

In general, excitation waves in the Tyson-Fife model can survive faster inhibitor diffusion – up to a certain point. The amount of u- and v-concentration in solution relies on an interplay between the spike in concentrations due to the traveling excitation wave and the diffusion of the two species. If a wave enters a regions in which the inhibitor species diffuses faster, it is possible for the trailing inhibitor peak to leak some inhibitor in front of the reaction front, as shown in Figure 1. This behavior should be

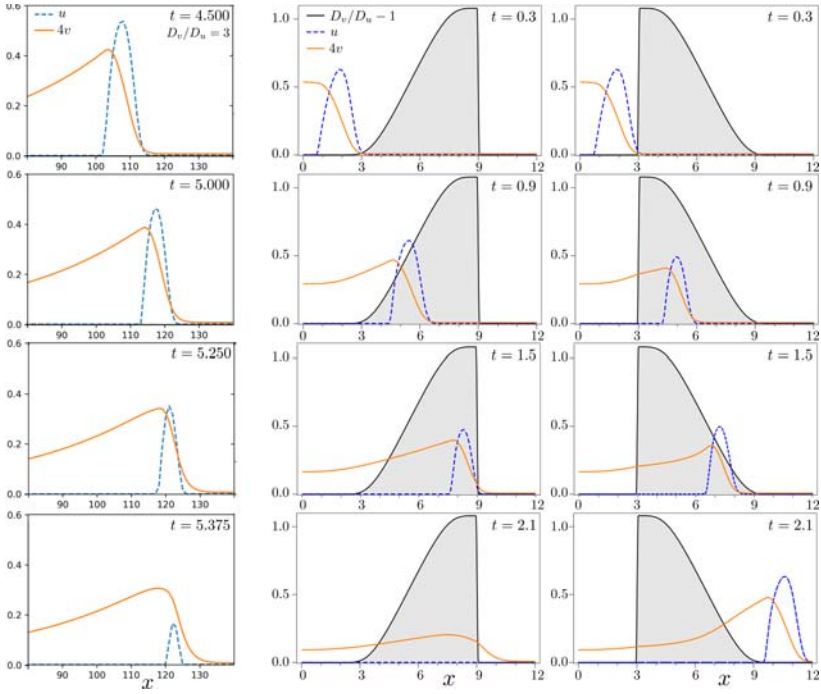

FIGURE 1
Fast Inhibitor Diffusion Region (FIDR) wavefront death. Left: FDM time series of an excitation wave propagating in a region with $D_v/D_u = 3.0$. The activator u concentration profile is dashed blue. The inhibitor v concentration profile is solid gold and has been multiplied by a factor of 4 for visualization. After the inhibitor concentration leaks into the front of the wave, the activator concentration quickly decreases. Center and Right: FEM time series of an excitation wave entering an FIDR gradient (gray area) with a diffusion-ratio of $y = (D_v/D_u) - 1$ (surrounded by $D_v/D_u = 1.0$). Center: wave survives propagation *down* an inhibitor diffusion gradient. Right: wave succumbs to propagation *up* an inhibitor diffusion gradient.

distinguished from a system where the inhibitor diffusion is larger throughout the system causing stationary Turing structures to appear [46].

The mechanism for wave death due to fast inhibitor diffusion suggests that the moment the inhibitor concentration increases above a certain value at the wave's front, the wave velocity decreases, allowing the inhibitor concentration to increase even further. At sufficiently large faster inhibitor diffusion, the wave dies before it can reach the end of the FIDR. Conversely, if a wave propagates into a high FIDR first, it slows down but can speed up again if the diffusion ratio is reduced before the wave dies.

Naturally, this behavior depends on the relative strength of the FIDR and the length of the region. For simplicity, we chose steps of equal height and

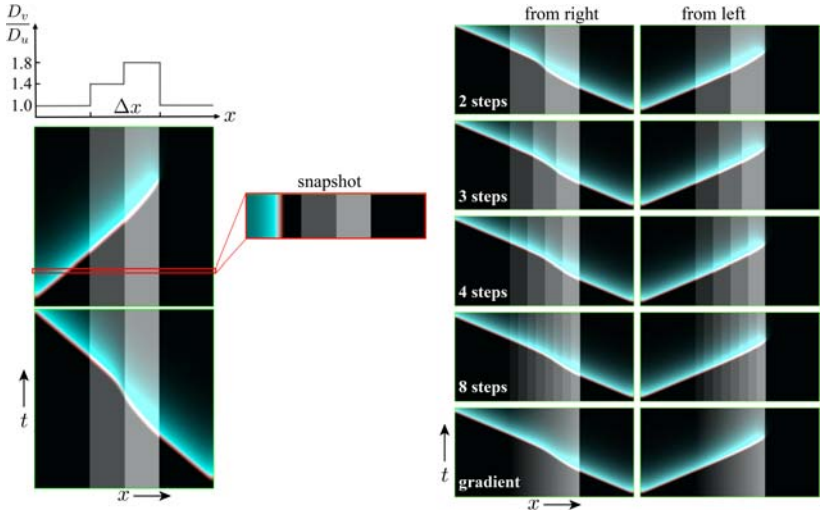

FIGURE 2
Fast Inhibitor Diffusion Region diodes. FDM time-space plots (time increasing upward) tracking activator u (red) and inhibitor v (blue) concentrations. Left: Two-step region diode with varying D_v/D_u showing wave entering from the left and dying before reaching the end of the diode (center) and wave entering from the right through the high step and successfully passing through the diode. Right: FDM time-space plots as excitation waves propagate through various step and gradient D_v distributions.

length. We compare the total width of the region to the characteristic wavelength of our excitable system. Our system exhibits non-monotonic dispersion, but under FDM successive wavefront peaks can be no closer than a characteristic wavelength $\lambda_c \approx 20$; under FEM and normal channel conditions, peak length $l \approx 2$ and diode length $\Delta x \approx 6$.

We constructed a quasi-1D, stepped region between two normal propagation regions where $D_v/D_u = 1.0$. An excitability drop via a step function is able to suppress wave propagation even if the same gradual excitability decrease would allow wave propagation [40]. The steps, from left to right, have diffusion ratios of $D_v/D_u = 1.4$ and $D_v/D_u = 1.8$, as shown on the left of Figure 2.

As outlined in the Introduction, there are a number of configurations and conditions for achieving unidirectional wave propagation in excitable reaction-diffusion systems. In the context of chemical computing, one-dimensional, one-way obstacles are desirable components for constructing logic gates. While diffusion-based unidirectional propagation has yet to be experimentally achieved, we believe that step-gradient diodes can be created by placing various gel segments in a row.

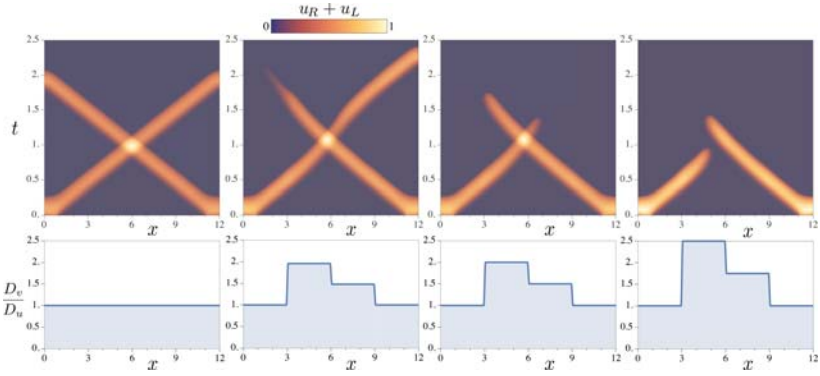

FIGURE 3
Two-step diode discovered by Finite Element Method (FEM) numerical integration of Tyson-Fife Eq. (4) with no-flux boundary conditions (cf. Fig 2 left). Top row: Time-space plots superimpose activator concentrations $u[x,t]$ for rightward and leftward waves. Bottom Row: Diffusion ratio plots indicate successively larger Fast Inhibitor Diffusion Region (FIDR) steps. Diode exists in second column, where the leftward wave dies due to D_v/D_u steps of just under ~ 0.5. For larger steps, both waves die. Smooth C^∞ steps constructed by superposing $e^{-1/x}$ functions.

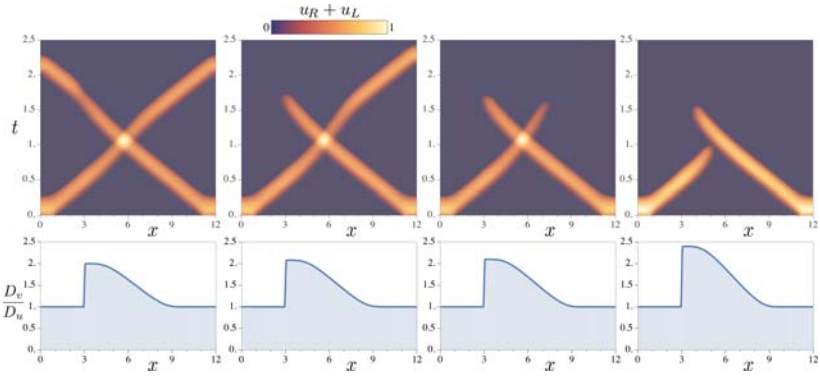

FIGURE 4
Gradient diode discovered by FEM numerical integration of Tyson-Fife Eq. (4) (cf. Figure 2 right). Top row: Time-space plots superimpose activator concentrations $u[x,t]$ for rightward and leftward waves. Bottom row: Diffusion ratio plots indicate successively larger FIDR gradients. Diode exists in second column, where the leftward wave dies due to the D_v/D_u gradient of just over $\sim 1.0/6.0$. For larger gradients, both waves die. Smooth C^∞ gradients constructed by superposing $e^{-1/x}$ functions.

For comparisons, we constructed FIDR in spatially symmetric channels and allowed RD-waves to enter the diode from either side. The right of Figure 2 shows a 2-step (top), a 4-step (middle), and a gradient (bottom) region with waves entering through the large step (left column) and small step (right

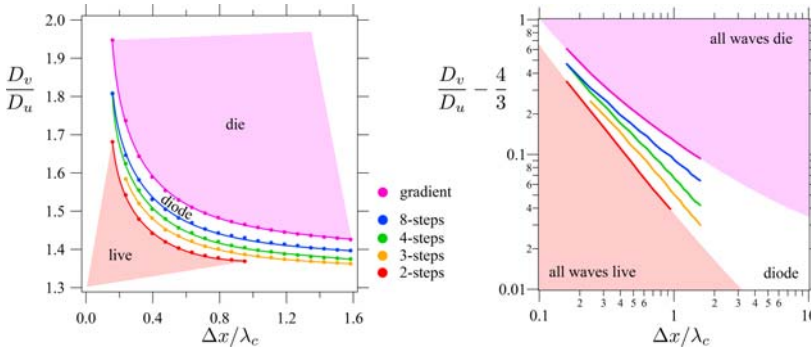

FIGURE 5
FDM diode exists between the red and magenta regions in linear-linear (left) and log-log (right) plots of diode maximum diffusion ratio D_v/D_u versus normalized diode length $\Delta x/\lambda_c$. For unidirectional propagation, short diodes need large excess inhibitor diffusion, while long diodes need small excess inhibitor diffusion.

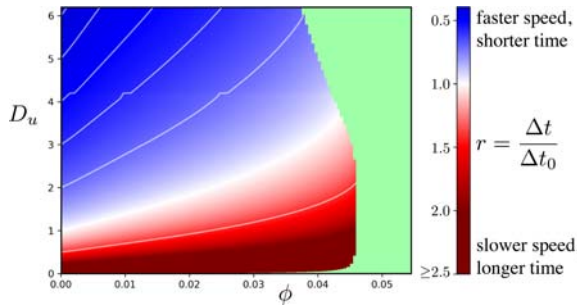

FIGURE 6
Control ratio r for different activator diffusions D_u and light intensities ϕ with no inhibitor diffusion ($D_v = 0$). Red-white-blue colors indicate FDM retardation compared to a normal wave with $D_u = 1$ and no illumination ($\phi = 0$). White indicates where illumination retardation balances diffusion advancement. For fixed activation diffusion, illumination increases retardation. Green indicates unsustainable or very slow propagation.

column). The figure also shows time-space plots of a wave propagating from the left and a wave propagating from the right. Clearly, one is able to traverse the obstacle and reach the other side of the channel and the other is not. In colloquial terms, the wave is unable to survive climbing up the steps but it is able to go down them. In addition to using the finite differencing method (FDM), we also applied the finite element method (FEM) and obtained very similar results for both the 2-step and the diffusion diodes, as illustrated by Figures 3 and 4.

Depending on the maximal D_u-value (total barrier height) waves can travel through the barrier from both sides, waves die entering from either side, or the one way travel of the diode effect obtains. According to Figure 5, for unidirectional propagation, short diodes need large excess inhibitor diffusion, while long diodes need small excess inhibitor diffusion, both for multi-step and gradient diodes.

4.2 Diffusion compensation

Since both light intensity ϕ and the diffusion rates D_u and D_v affect the speed of an excitation wave, it is possible to compensate one effect by the other as they act in opposite directions. A similar illumination compensation of waves propagating through a non-planar system has been reported by Kheowan *et al.* [20].

To explore diffusion compensation by light, we simulate wave propagation in one-dimensional channels and record the time for waves to traverse them. Normal control conditions of $D_u = 1.0$, $D_v = 0.0$ and $\phi = 0.0$ fix the default time. Other combinations of D_u, $D_v = 0$, and ϕ generate different times (with an immobilized gel maintaining zero inhibitor diffusion). To quantify the advancement or delay of propagating waves, we introduce the control ratio or retardation $r = \Delta t / \Delta t_0$, where Δt is the time for a wave to traverse the path under specific diffusion D_u and light ϕ divided by the time Δt_0 for the control wave to traverse the path.

Figure 6 plots the control ratio versus activator diffusion and illumination. Distinct regions include: i) The upper left, blue region where the wave is faster than the control wave due to the faster activator diffusion; ii) The lower right, red region where the wave is slower than the control wave due to the smaller D_u value; iii) The white line that separates the faster region and the slower wave region highlighting the non-trivial compensation relationship; iv) The upper right region with unsustainable conditions and wave death within the channel; and v) The cusp in the bottom right corner of the graph at the border of the green region of unsustainable wave propagation has an interesting, curved or feathered appearance.

Figure 6 is based on simulation data using Obj-C when we created a path of a certain length and determined the time it would take a 1D wave to traverse it. The figure is the result of two separate simulations in which we used different time steps in both data frames, due to computer limitations. For simulations with $D_u < 4.2$ we used $\Delta s = 0.125$ and $\Delta t = 0.00188$. For simulations with $D_u \geq 4.2$ we used $\Delta s = 0.15$ and $\Delta t = 0.0002$. As a result, a slight shift in the gray contours is at $D_u = 4.2$.

4.3 Chemical computing on/off switch

The diffusion diode also enables the creation of a very energy efficient on/off-switch for chemical computation circuits in which a low intensity light pulse

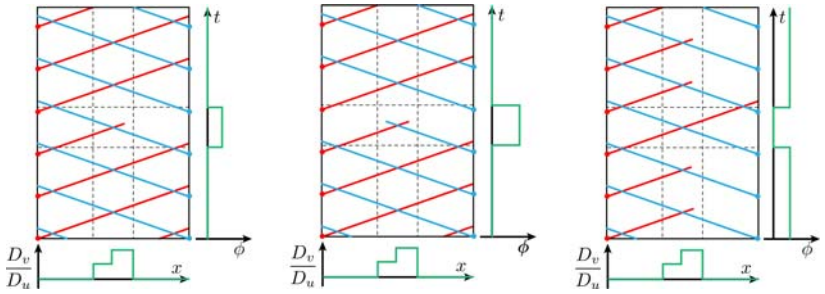

FIGURE 7
Schematic time-space plots of periodic reaction diffusion waves with variable diffusion D_v / D_u and illumination ϕ illustrate light switches. Leftward (red) and rightward (blue) waves are independent experiments. Left: Faint light increase creates a diode. Middle: Strong light pulse destroys the diode and creates a 2-way barrier. Right: Faint light decrease destroys a diode and creates a 2-way opening.

can be applied to disable the successful wave propagation. If the system conditions allow a wave to barely make it through the diffusion diode, a very weak light pulse is sufficient to suppress the transmission through the diode. This is energetically more favorable than applying a strong light pulse to eliminate the wave.

On the other hand, it is possible to disable a diffusion diode (make it passable in both direction), if the system is constantly illuminated. By reducing the light intensity slightly for a short period of time, it would be possible to 'open' the diode for a wave to pass through. Instead of turning off the light completely to allow such a behaviour, the illumination only changes slightly, creating a less flickering set-up, which can increase the life-time of the used light sources. Figure 7 schematically illustrates some light switches.

5 CONCLUSION

We have numerically investigated the propagation of chemical reaction-diffusion waves through narrow, quasi-one-dimensional channels. In Fast Inhibitor Regions, two-variable reaction diffusion waves die due to the inhibitor concentration that is classically responsible for the refractory period outspeeding the activation front and destroying the excitation.

Unidirectional propagation is observed to occur with obstacles of increasing inhibitor diffusion rates. Going up the obstacle damages the wavefront to the point where it cannot successfully propagate across the soft obstacle. On the other hand, a healthy wave can survive the extreme diffusion ratio when going down the obstacle.

We observe a kind of diffusion ratio forgiveness for a particular obstacle length. Diode behavior with two step obstacles requires particular diffusion ratios, while gradient obstacles display unidirectional behavior for a host of ratios for the same obstacle length. This suggests that gradient diodes would be more forgiving to achieve experimentally, but stepped diodes (e.g., horizontal layers of different gel densities) may be more practical to execute.

ACKNOWLEDGMENTS

This work was supported by the National Science Foundation (NSF grant DMR-1852095), the Sherman-Fairchild Foundation, the Koontz Endowed Fund, and The College of Wooster.

REFERENCES

[1] (2020). Mathematica. Wolfram Research, Inc.

[2] Andrew Adamatzky. (January 2020). On interplay between excitability and geometry. *Biosystems*, 187:104034.

[3] Andrew Adamatzky, Ben De Lacy Costello, and Tetsuya Asai. (2005). *Reaction-Diffusion Computers*. Elsevier, Amsterdam; Boston. OCLC: 162586833 https://doi.org/10.1016/B978-0-444-52042-5.X5000-2.

[4] Konstantin I. Agladze, Rubin R. Aliev, Tomohiko Yamaguchi, and Kenichi Yoshikawa. (January 1996). Chemical Diode. *The Journal of Physical Chemistry*, 100(33):13895–13897.

[5] Gavin R. Armstrong, Annette F. Taylor, Stephen K. Scott, and Vilmos Gáspár. (2004). Modelling wave propagation across a series of gaps. *Physical Chemistry Chemical Physics*, 6(19):4677–4681.

[6] Agnessa Babloyantz and J.A. Sepulchre. (April 1991). Target and spiral waves in oscillatory media in the presence of obstacles. *Physica D: Nonlinear Phenomena*, 49(1-2):52–60.

[7] Dwight Barkley. (April 1991). A model for fast computer simulation of waves in excitable media. *Physica D: Nonlinear Phenomena*, 49(1-2):61–70.

[8] Marta Dueñas-Díez and Juan Pérez-Mercader. (September 2019). How Chemistry Computes: Language Recognition by Non-Biochemical Chemical Automata. From Finite Automata to Turing Machines. *iScience*, 19:514–526.

[9] G. Bard Ermentrout and John Rinzel. (August 1996). Reflected Waves in an Inhomogeneous Excitable Medium. *SIAM Journal on Applied Mathematics*, 56(4):1107–1128.

[10] Richard J. Field and Richard M. Noyes. (March 1974). Oscillations in chemical systems. IV. Limit cycle behavior in a model of a real chemical reaction. *The Journal of Chemical Physics*, 60(5):1877–1884.

[11] Xiang Gao, Alexei Krekhov, Vladimir S. Zykov, and Eberhard Bodenschatz. (February 2018). Initiation of Rotors by Fast Propagation Regions in Excitable Media: A Theoretical Study. *Frontiers in Physics*, 6:8.

[12] Vilmos Gáspár, G. Bazsa, and M. T. Beck. (1983). The influence of visible light on the Belousov-Zhabotinskii oscillating reactions applying different catalysts. *Zeitschrift für Physikalische Chemie*, 264(1):43–48.

[13] Joanna N. Gorecka, Jerzy Gorecki, and Yasuhiro Igarashi. (February 2007). One Dimensional Chemical Signal Diode Constructed with Two Nonexcitable Barriers. *The Journal of Physical Chemistry A*, 111(5):885–889.

[14] Jerzy Gorecki, Konrad Gizynski, Jan Guzowski, Joanna N. Gorecka, Piotr Garstecki, Gerd Gruenert, and Peter Dittrich. (July 2015). Chemical computing with reaction-diffusion processes. *Philosophical Transactions of the Royal Society A: Mathematical, Physical and Engineering Sciences*, 373(2046):20140219.

[15] Jerzy Gorecki and Joanna N. Gorecka. (2018). Computing in geometrical constrained excitable chemical systems. In Andrew Adamatzky, editor, *Unconventional Computing: A Volume in the Encyclopedia of Complexity and Systems Science, Second Edition*, pages 195–223. Springer US, New York, NY.

[16] Jerzy Gorecki, Joanna N. Gorecka, and Y. Igarashi. (September 2009). Information processing with structured excitable medium. *Natural Computing*, 8(3):473–492.

[17] Takatoshi Ichino, Kenji Fujio, Mariko Matsushita, and Satoshi Nakata. (March 2009). Wave propagation in the photosensitive belousov–zhabotinsky reaction across an asymmetric gap. *The Journal of Physical Chemistry A*, 113(11):2304–2308.

[18] Takatoshi Ichino, Yasuhiro Igarashi, Ikuko N. Motoike, and Kenichi Yoshikawa. (May 2003). Different operations on a single circuit: Field computation on an excitable chemical system. *The Journal of Chemical Physics*, 118(18):8185–8190.

[19] Raymond Kapral and Kenneth Showalter, editors. (1995). *Chemical Waves and Patterns*. Springer Netherlands, Dordrecht.

[20] On-Uma Kheowan, Vasily A. Davydov, Niklas Manz, and Stefan C. Müller. (July 2007). Compensation of curvature effects by illumination. *Physics Letters A*, 367(4-5):311–315.

[21] Michal Kozák, Eamonn A. Gaffney, and Václav Klika. (October 2019). Pattern formation in reaction-diffusion systems with piecewise kinetic modulation: An example study of heterogeneous kinetics. *Physical Review E*, 100(4):042220.

[22] Hans-Jürgen Krug, Hermann Brandtstädter, and Ludwig Pohlmann. (June 1995). Nucleation and Wave Propagation in the Modified Oregonator and Comparison with Experiments in a Photosensitive Belousov–Zhabotinsky Gel Reactor. *The Journal of Physical Chemistry*, 99(25):10237–10245.

[23] Lothar Kuhnert. (January 1986). A new optical photochemical memory device in a light-sensitive chemical active medium. *Nature*, 319(6052):393–394.

[24] Lothar Kuhnert, Hans-Jürgen Krug, and Ludwig Pohlmann. (May 1985). Velocity of trigger waves and temperature dependence of autowave processes in the Belousov–Zhabotinsky reaction. *The Journal of Physical Chemistry*, 89(10):2022–2026.

[25] Claudia Lenk, Mario Einax, J. Michael Köhler, and Philipp Maass. (February 2019). Complex oscillation modes in the Belousov–Zhabotinsky reaction by weak diffusive coupling. *Physical Review E*, 99(2):022202.

[26] Ilya L. Mallphanov and Vladimir K. Vanag. (January 2020). Fabrication of New Belousov–Zhabotinsky Micro-Oscillators on the Basis of Silica Gel Beads. *The Journal of Physical Chemistry A*, 124(2):272–282.

[27] Jerzy Maselko, John S. Reckley, and Kenneth Showalter. (April 1989). Regular and irregular spatial patterns in an immobilized-catalyst Belousov-Zhabotinskii reaction. *The Journal of Physical Chemistry*, 93(7):2774–2780.

[28] František Muzika and Jerzy Górecki. (February 2022). Identification of the best medium for experiments on chemical computation with Belousov–Zhabotinsky reaction and ferroin-loaded Dowex beads. *Reaction Kinetics, Mechanisms and Catalysis*.

[29] Carl Neumann. (December 1877). Zur Theorie des Logarithmischen und des Newton'schen Potentials (On the theory of logarithmic and Newtonian potential). *Mathematische Annalen*, 11(4):558–566.

[30] Arcady V. Pertsov, E. A. Ermakova, and Emmanuil E. Shnol. (August 1990). On the diffraction of autowaves. *Physica D: Nonlinear Phenomena*, 44(1-2):178–190.

[31] Maria S. Poptsova and Georgy T. Guria. (September 1997). Autowave tunneling through a non-excitable area of active media. *General Physiology and Biophysics*, 16(3):241–261.

[32] Zahra Rostami, Karthikeyan Rajagopal, Abdul Jalil M. Khalaf, Sajad Jafari, Matjaž Perc, and Mitja Slavinec. (November 2018). Wavefront-obstacle interactions and the initiation of reentry in excitable media. *Physica A: Statistical Mechanics and its Applications*, 509:1162–1173.

[33] Irene Sendiña-Nadal, Maite de Castro, Francesc Sagués, and Moncho Gómez-Gesteira. (July 2002). Unidirectional mechanism for reentrant activity generation in excitable media. *Physical Review E*, 66(1):016215.

[34] Irene Sendiña-Nadal, M. deCastro, and Moncho Gómez-Gesteira. (2006). Kinematic description of wave propagation through a chemical diode. *Chaos: An Interdisciplinary Journal of Nonlinear Science*, 16(3):033110.

[35] Hana Ševčíková and Miloš Marek. (October 1983). Chemical waves in electric field. *Physica D: Nonlinear Phenomena*, 9(1-2):140–156.

[36] Nathaniel J. Smith, Rebecca Glaser, Vincent W. H. Hui, John F. Lindner, and Niklas Manz. (March 2019). Disruption and recovery of reaction-diffusion wavefronts colliding with obstacles. *Physica A: Statistical Mechanics and its Applications*, 517:307–320.

[37] Oliver Steinbock, Ágota Tóth, and Kenneth Showalter. (February 1995). Navigating Complex Labyrinths: Optimal Paths from Chemical Waves. *Science*, 267(5199):868–871.

[38] Ming-Zhu Sun and Xin Zhao. (March 2013). Multi-bit binary decoder based on Belousov–Zhabotinsky reaction. *The Journal of Chemical Physics*, 138(11):114106.

[39] Masanobu Tanaka, Marcel Hörning, Hiroyuki Kitahata, and Kenichi Yoshikawa. (October 2015). Elimination of a spiral wave pinned at an obstacle by a train of plane waves: Effect of diffusion between obstacles and surrounding media. *Chaos: An Interdisciplinary Journal of Nonlinear Science*, 25(10):103127.

[40] Masanobu Tanaka, Hiroki Nagahara, Hiroyuki Kitahata, Valentin I. Krinsky, Konstantin I. Agladze, and Kenichi Yoshikawa. (July 2007). Survival versus collapse: Abrupt drop of excitability kills the traveling pulse, while gradual change results in adaptation. *Physical Review E*, 76(1):016205.

[41] Masahiro Toiya, Vladimir K. Vanag, and Irving R. Epstein. (September 2008). Diffusively Coupled Chemical Oscillators in a Microfluidic Assembly. *Angewandte Chemie International Edition*, 47(40):7753–7755.

[42] Ágota Tóth, Vilmos Gáspár, and Kenneth Showalter. (January 1994). Signal transmission in chemical systems: Propagation of chemical waves through capillary tubes. *The Journal of Physical Chemistry*, 98(2):522–531.

[43] Ágota Tóth, Dezső Horváth, and Kenichi Yoshikawa. (September 2001). Unidirectional wave propagation in one spatial dimension. *Chemical Physics Letters*, 345(5-6):471–474.

[44] Ágota Tóth and Kenneth Showalter. (August 1995). Logic gates in excitable media. *The Journal of Chemical Physics*, 103(6):2058–2066.

[45] Sonja Totz, Jakob Löber, Jan Frederik Totz, and Harald Engel. (May 2018). Control of transversal instabilities in reaction-diffusion systems. *New Journal of Physics*, 20(5):053034.

[46] Alan M. Turing. (August 1952). The chemical basis of morphogenesis. *Philosophical Transactions of the Royal Society of London. Series B, Biological Sciences*, 237(641):37–72.

[47] John J. Tyson and Paul C. Fife. (September 1980). Target patterns in a realistic model of the Belousov-Zhabotinskii reaction. *The Journal of Chemical Physics*, 73(5):2224–2237.

[48] Vladimir K. Vanag and Irving R. Epstein. (July 2004). Subcritical wave instability in reaction-diffusion systems. *The Journal of Chemical Physics*, 121(2):890–894.

[49] Guo-Mao Zhang, Ieong Wong, Meng-Ta Chou, and Xin Zhao. (April 2012). Towards constructing multi-bit binary adder based on Belousov–Zhabotinsky reaction. *The Journal of Chemical Physics*, 136(16):164108.

[50] Vladimir S. Zykov. (December 2018). Spiral wave initiation in excitable media. *Philosophical Transactions of the Royal Society A: Mathematical, Physical and Engineering Sciences*, 376(2135):20170379.

[51] Vladimir S. Zykov and Eberhard Bodenschatz. (March 2018). Wave propagation in inhomogeneous excitable media. *Annual Review of Condensed Matter Physics*, 9(1):435–461.

[52] Vladimir S. Zykov, Alexei Krekhov, and Eberhard Bodenschatz. (February 2017). Fast propagation regions cause self-sustained reentry in excitable media. *Proceedings of the National Academy of Sciences*, 114(6):1281–1286.